Protein Science (1995), *4*:1081–1087. Cambridge University Press. Printed in the USA.

Three-dimensional structure of the complex of 4-guanidino-Neu5Ac2en and influenza virus neuraminidase

JOSEPH N. VARGHESE, V. CHANDANA EPA, AND PETER M. COLMAN
Biomolecular Research Institute, Parkville, Victoria 3052, Australia

(RECEIVED January 4, 1995; ACCEPTED March 15, 1995)

Abstract

The three-dimensional X-ray structure of a complex of the potent neuraminidase inhibitor 4-guanidino-Neu5Ac2en and influenza virus neuraminidase (Subtype N9) has been obtained utilizing diffraction data to 1.8 Å resolution. The interactions of the inhibitor, solvent water molecules, and the active site residues have been accurately determined. Six water molecules bound in the native structure have been displaced by the inhibitor, and the active site residues show no significant conformational changes on binding. Sialic acid, the natural substrate, binds in a half-chair conformation that is isosteric to the inhibitor. The conformation of the inhibitor in the active site of the X-ray structure concurs with that obtained by theoretical calculations and validates the structure-based design of the inhibitor. Comparison of known high-resolution structures of neuraminidase subtypes N2, N9, and B shows good structural conservation of the active site protein atoms, but the location of the water molecules in the respective active sites is less conserved. In particular, the environment of the 4-guanidino group of the inhibitor is strongly conserved and is the basis for the antiviral action of the inhibitor across all presently known influenza strains. Differences in the solvent structure in the active site may be related to variation in the affinities of inhibitors to different subtypes of neuraminidase.

Keywords: active site; anti-influenza drugs; crystallography; inhibitor binding; neuraminidase

The enzyme neuraminidase (reviewed by Colman, 1989) is one of two membrane-bound glycoproteins found on the surface of influenza virus. The other is hemagglutinin, which binds to α-ketosidically linked terminal sialic acid on the receptor molecules of target cells and fuses the viral membrane with an endosomal membrane. Neuraminidase, which removes terminal sialic acid from a range of glycoconjugates, plays an important role in facilitating the spread of viral infection. By removing terminal sialic acid from the mucous layer protecting target cells, neuraminidase may facilitate penetration of the virus to the target cell surface. Neuraminidase activity is also required to release progeny virions from the surface of infected cells. Inhibition of this glycohydrolase can provide a means of controlling influenza infections.

The X-ray molecular structure of influenza virus neuraminidase has been determined (Varghese et al., 1983; Baker et al., 1987; Tulip et al., 1991; Varghese & Colman, 1991; Burmeister et al., 1992). The active site is a pocket lined by amino acids that are conserved in all known strains of influenza virus (Colman et al., 1983). This conserved active site pocket is surrounded by highly strain-variable surface residues (Fig. 1) that ensure that the virus remains antigenically viable. The footprint of an antibody in the antigen–antibody interface site is larger than the exposed surface of the conserved region of the active site (Colman et al., 1987, 1989). The virus is thus able to overcome host immune pressure by mutation of residues that do not have a catalytic or structural role (Varghese et al., 1988; Tulip et al., 1991) but are able to disrupt the antigen–antibody binding interface.

New inhibitors of the enzyme (von Itzstein et al., 1993) have been designed on the basis of the knowledge of enzyme structure and the mode of binding of substrate, sialic acid, and substrate analogues, Neu5Ac2en (Varghese et al., 1992). These new inhibitors affect replication of the virus in vitro and in animal models through an intranasal route of administration. They are effective as enzyme inhibitors against all currently known strains of influenza but show slight variations in K_i from strain to strain. Differences in the binding constants must arise from slight differences in the detailed geometry of the active site, including the structure and role of water molecules in the active site. Here we describe the high-resolution X-ray structure of in-

Reprint requests to: Joseph N. Varghese, Biomolecular Research Institute, 343 Royal Parade, Parkville, Victoria 3052, Australia; e-mail: jose@venus.dbe.csiro.mel.au.

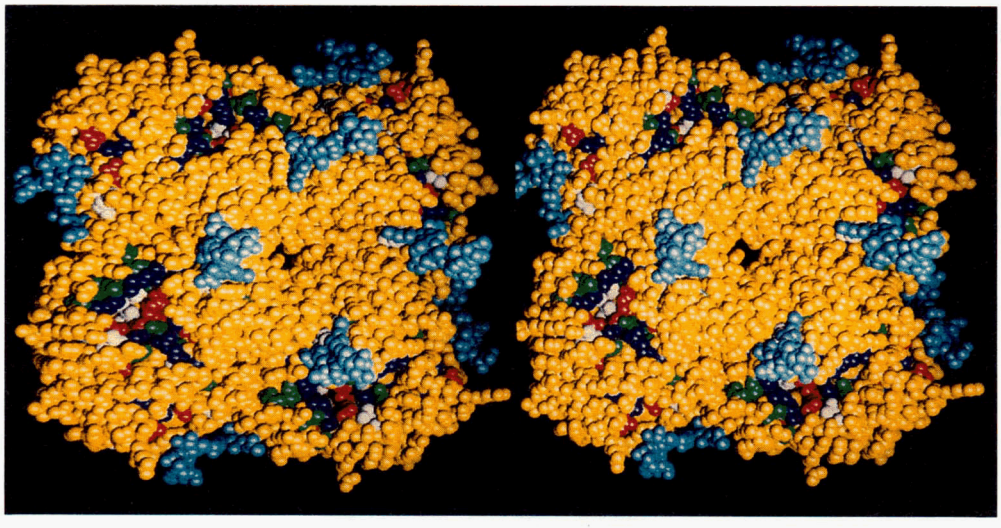

Fig. 1. Stereo image of a CPK atomic model of an influenza virus neuraminidase tetrameric head viewed distal to viral membrane. Atoms colored yellow belong to residues that vary among known sequences of the enzyme; in light blue are N-linked carbohydrate residues; the remaining atoms are those of totally conserved residues, which for the most part are in the active site pocket of the molecule. Blue, red, white, and green represent conserved basic, acidic, neutral, and hydrophobic amino acids, respectively. The tri-arginyl cluster in the active site is located in the upper side of the active site on the bottom right subunit.

fluenza subtype N9 neuraminidase in complex with 4-guanidino-Neu5Ac2en and compare it with that obtained by a molecular mechanics energy minimization of the structure.

Results

The location of 4-guanidino-Neu5Ac2en moiety in the active site of N9 neuraminidase is as found in N2 neuraminidase (A/Tokyo/3/67) (von Itzstein et al., 1993). The increased accuracy of the N9 neuraminidase complex has unambiguously resolved the orientation of the inhibitor and confirmed the hydrogen bonding pattern of the 4-guanidino group. All the atoms in the inhibitor and the structural waters are clearly resolved in the final electron density map (Fig. 2).

Inhibitor–active site interactions

Apart from the additional interactions formed by the 4-guanidino group, interactions of other atoms of the inhibitor with the N9 neuraminidase active site are similar to those found in N2 (Varghese et al., 1992) and type B (Burmeister et al., 1992) neuraminidase complexes with Neu5Ac2en (Fig. 3). An N9/Neu5Ac2en complex (Bossart-Whitaker et al., 1993) has not been examined in this comparison because it was done at low resolution with no structural waters in the active site. One of the primary guanidinyl nitrogens is hydrogen bonded to the main-chain oxygen at residue 178 (N2 sequence numbering), a carboxylate oxygen of Glu 227, and a water molecule. The other primary guanidinyl nitrogen interacts with the main chain car-

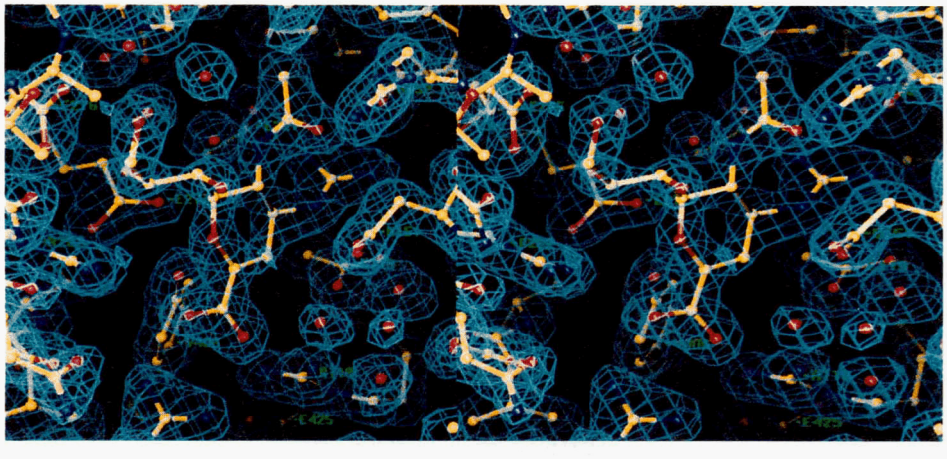

Fig. 2. Stereo image of a $2F_o - F_c$ electron density map (cage mesh contour at 1.5σ) of the active site of N9 neuraminidase complexed with 4-guanidino-Neu5Ac2en (at center of picture) superimposed with the final refined atomic structure (ball and stick representation). F_o and F_c are the observed and calculated X-ray structure factors and phases are from the final refined atomic model. Water molecules are represented by red spheres.

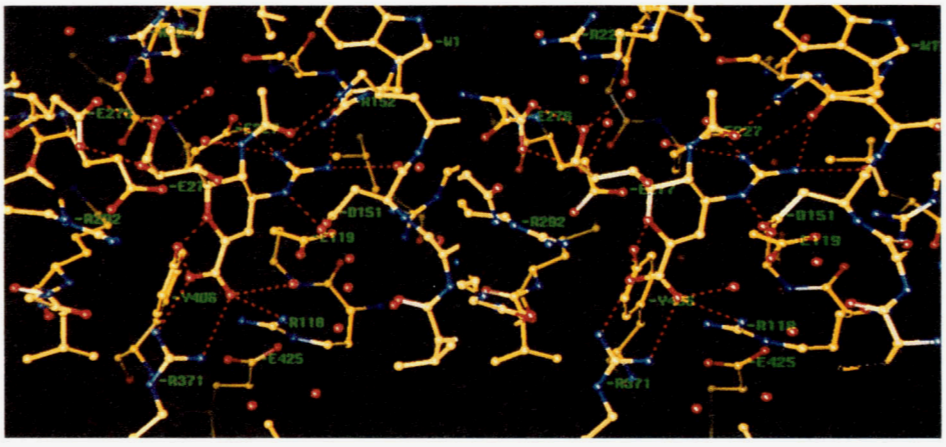

Fig. 3. Stereo image of the hydrogen bonding pattern of 4-guanidino-Neu5Ac2en in the active site of N9 neuraminidase. All nonbonded contacts between polar atoms of the inhibitor and the protein less than 3.2 Å are drawn in red dotted lines.

bonyl oxygens of residues 178 and 151. The secondary guanidinyl nitrogen of the 4-guanidinyl group interacts with the carboxylate of Glu 119 and Asp 151. The interaction with Glu 119 lacks the necessary hydrogen bonding geometry, as the carboxylate group of Glu 119 stacks parallel to the guanidinyl group (Fig 3). In this case the interactions are electrostatic and van der Waals in character.

Theoretical inhibitor–active site interactions

During the design phase of the 4-guanidino-Neu5Ac2en inhibitor, von Itzstein et al. (1993) predicted a different binding mode of the 4-guanidinyl group of the inhibitor in the active site of N2 neuraminidase. The guanidinyl group was rotated with respect to the X-ray result, resulting in additional H-bonding interactions with Glu 119. In order to explore the possibility of alternative modes of H-bonding of the guanidinium moiety in the active site, energy minimized structures were calculated using AMBER (Pearlman et al., 1990) based on two different starting models for the dihedral angle (see the Materials and methods). Initially, minimization allowing the protein non-hydrogen atoms to relax resulted in unacceptably large change in the protein structure. In particular, the Cδ of glutamate 119 and 277 shifted by 0.41 Å and the Cζ of Tyr 406 was displaced 0.57 Å. The movement of Glu 119 allowed formation of a hydrogen bond with the 4-guanidinyl group, for which the dihedral angle refined to 188° and was independent of its starting value of 172° (in the X-ray structure) or 220°. For these reasons, the minimizations were repeated as described in the Materials and methods, with the non-hydrogen atoms of the protein fixed. Both starting models (dihedral angles 172° and 220°) refined to a structure in which the dihedral angle is 169° and in which no hydrogen bonding occurs between Glu 119 and the inhibitor (Fig. 4).

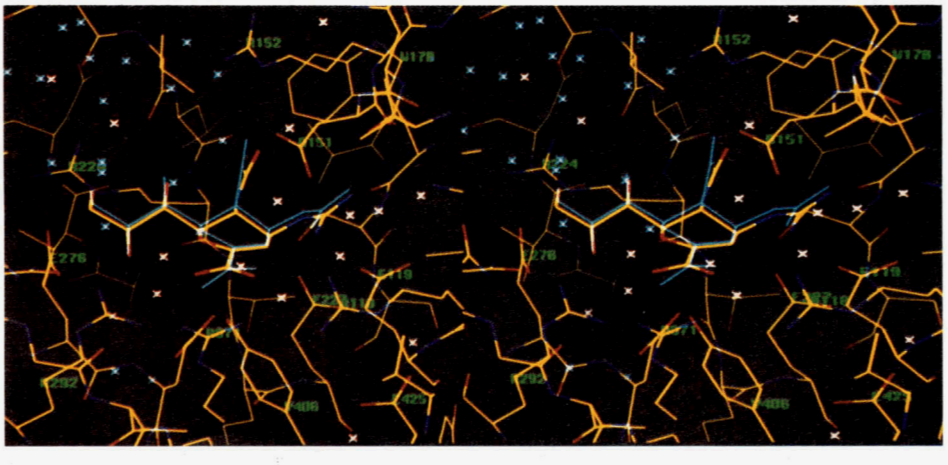

Fig. 4. Stereo image of the environment of the 4-guanidino group of 4-guanidino-Neu5Ac2en in the conserved pocket of N9 neuraminidase. The X-ray model (color) is superimposed with the theoretical energy-minimized model (light blue) where the protein non-hydrogen atoms were "frozen" at their X-ray positions. White crosses represent crystallographic water molecules used in the theoretical model. Blue crosses are additional "theoretical" water molecules.

Discussion

The refined, high-resolution structure described here confirms that 4-guanidino-Neu5Ac2en binds to the active site of influenza virus neuraminidase isosterically with the parent inhibitor Neu5Ac2en. Furthermore, the additional interactions due to the replacement of the 4-hydroxyl group of Neu5Ac2en with the guanidinyl side chain are via hydrogen bonds to Glu 227, Asp 151, and a peptide carbonyl, and via an ionic, non-H-bonded link to Glu 119. Earlier modeling of the interaction between 4-guanidino-Neu5Ac2en and the protein had led to the conclusion that H-bonds would form with Glu 119 (von Itzstein et al., 1993). This X-ray experiment shows this not to be the case. The experimental result can be duplicated computationally provided that the protein is held to the structure observed in the uncomplexed form. In many systems, ligand binding causes changes to the protein structure and modeling such changes may be critical for predicting binding interactions. Significant difficulties are still experienced in correctly modeling even modest changes to the structure, such as the replacement of a hydroxyl with a guanidinyl as in this example.

The native structure (Fig. 5), when compared with the inhibitor complex, shows six water molecules have been displaced: two at the carboxylate end, one near C4 of the pyranose ring, two near C9 of the 6-glycerol side chain, and one at the 4-guanidino group. There is also some rearrangement of the water structure. There is virtually no change in the orientation of the active site amino acid side chains, except for minor conformational changes in Glu 276 and Arg 224. The Asp 151 carboxylate group has rotated slightly to form a hydrogen bond with one of the nitrogens on the 4-guanidino group. The two water molecules near the 2-carboxylate group oxygens may be statistically occupied in the crystal lattice as they are only 2.53 Å apart.

An analysis of the active sites (Fig. 6) of N2 (Varghese & Colman, 1991), N9 (this paper), and B (Burmeister et al., 1992) show that there are no significant differences between the active site side-chain orientations, except some minor displacements in the region around Arg 224 and Glu 276, where the major interactions of the 6-glycerol group of Neu5Ac2en occur. However, there are differences in the water structure. This could be due to different crystallization conditions in the three structures or to a second order effect reflecting differences in the nonconserved residues neighboring the active site. Gly 405 (in N2 and N9) is replaced by a tryptophan in type B neuraminidase and displaces four water molecules that lie in a solvent pocket bounded by Arg 371 and Arg 118. Val 240 (in N2 and N9) is replaced by a methionine in type B and displaces two bound water molecules that form a channel under Arg 224 in the type A structures. These waters are not displaced by the inhibitor in N9 but would alter the hydrogen bonding pattern of the water molecules in the active site of type B compared with type A. An analysis of the water structure in type B indicates that most of the active site water molecules are in a similar location to those found in N9, and the largest differences in position are near the nonconserved regions of the active site pocket. The different K_i's reported for 4-guanidino-Neu5Ac2en with the N2, N9, and B neuraminidases (Pegg & von Itzstein, 1994) may reflect differences in the binding energy of the displaced water molecules in the active site; however, recent studies (Hart & Bethell, 1995) indicate that the association and dissociation rate constants for both A and B influenza neuraminidases are almost identical.

The specificity of 4-guanidino-Neu5Ac2en to influenza virus neuraminidase (von Itzstein et al., 1993) arises from the conservation in all viral neuraminidases of amino acids in the pocket in which the 4-guanidinyl group is located, in particular, Glu 119 and Glu 227. In bacterial neuraminidase structures (Crennell et al., 1993, 1994), these glutamyl residues are replaced by isoleucine and valine, respectively. The 4-hydroxyl binding pocket in these bacterial neuraminidases is formed by one aspartyl residue and one arginyl residue, and the homologues of these amino acids in the influenza virus neuraminidase are Ser 179 and Gln 136, respectively. Thus, the bacterial enzyme has neither shape nor chemical characteristics that permit tight binding of 4-guanidino-Neu5Ac2en.

There is considerable structural conservation between the influenza neuraminidases and the bacterial sialidases at the carboxy-

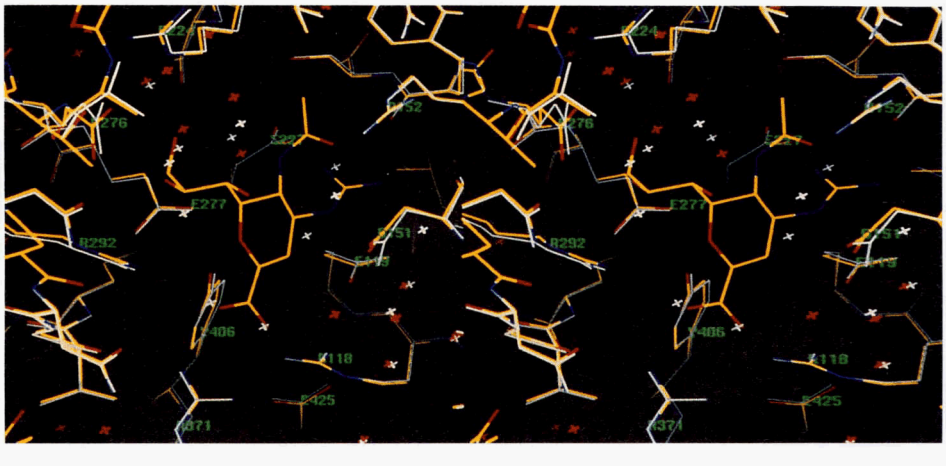

Fig. 5. Stereo image of the native N9 active site (light blue) superimposed with the inhibitor complex (color), showing the water structure of the uncomplexed and complexed structures as white and red crosses, respectively, and illustrating the small conformational changes in the protein on binding to the inhibitor.

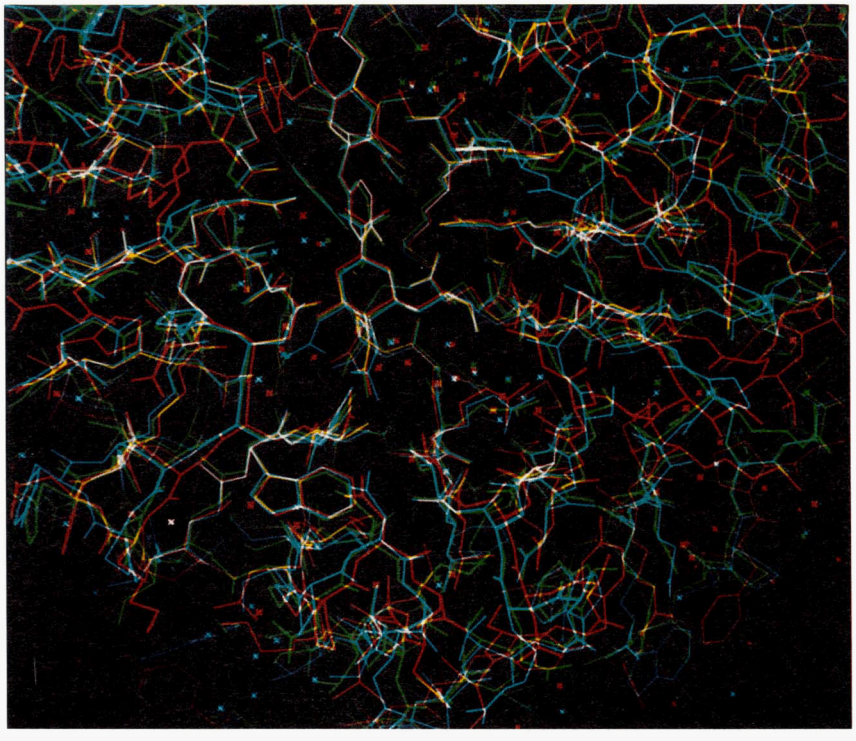

Fig. 6. View into the active site of the N9 neuraminidase (light blue) complexed with 4-guanidino-Neu5Ac2en and N2 (green) complexed with sialic acid (Varghese & Colman, 1991) of type A influenza and influenza type B (red) (Burmeister et al., 1991). The molecules have been superimposed by O (Jones et al., 1991) using every Cα atom in the structure and not including the inhibitor. Note the structural conservation of the active site and the variability of the rest of the molecule. The tri-arginyl cluster in the active site is located at the bottom half of the figure.

late-binding end of the catalytic site. The residues Asp 151, Arg 118, Glu 277, Arg 292, Val (or Ile) 349, Arg 371, Tyr 406, and Glu 425 are conserved in known viral and bacterial neuraminidase structures. The argininyl residues 118, 371, and 292 position the 2-carboxylate group and Val (or Ile) 349, Glu 425, and Glu 277 are important in positioning the tri-arginyl cluster. Asp 151 and Tyr 406 are presumably important in bond cleavage, but the precise mechanism is still unclear.

These eight residues (Fig. 7) are thus most likely to be conserved in all neuraminidases, and differences between viral, bac-

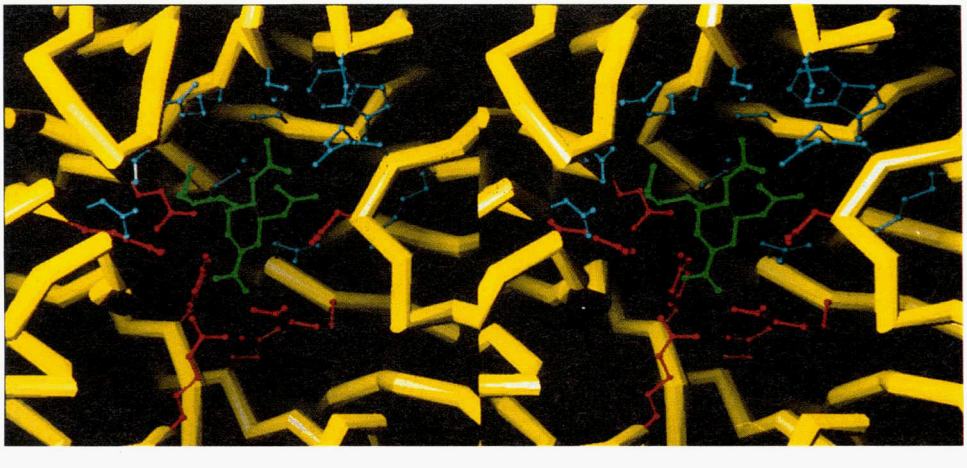

Fig. 7. Stereo image of the active site of Tern/N9 showing the active site residues surrounding 4-guanidino-Neu5Ac2en (green). Those residues that are conserved in influenza neuraminidase and bacterial neuraminidase are colored in red (R118, D151, E277, R292, R371, Y406, ED425), and those that are conserved only in influenza virus are colored in light blue (E119, R152, R156, W178, S179, D198, I222, R224, E227, E276, N294). The Cα backbone is represented by a yellow tube.

terial, and mammalian neuraminidase structures, arising from differences in the roles these enzymes have in vivo, are likely to be in the interactions of the 6-glycerol, 5-*N*-acetyl, and 4-OH groups of sialic acid. In the case of influenza virus neuraminidase, the turnover rate must be balanced against the requirement to maintain sufficient sialic acid at the cell surface to enable attachment via the hemagglutinin. This balance may require some configuration of residues in the active site not directly responsible for catalysis but only involved in the binding and release of sialic acid.

The 4-guanidino-Neu5Ac2en inhibitor is currently undergoing clinical trials, and initial results from a double-blind, randomized, placebo-controlled trial using this compound have been successful both for early treatment and prophylaxis of experimental inoculation of human volunteers with influenza A/Texas/91 (H1N1) (Hayden et al., 1994).

Materials and methods

Data collection

Neuraminidase enzyme was purified from influenza virus A/tern/Australia/G70C/75 as described previously (McKimm-Breschkin et al., 1991) and crystallized by established procedures (Laver et al., 1984). Crystals were soaked for 2 days in 40 mM 4-guanidino-Neu5Ac2en, and data were collected to 1.8 Å on the Weissenberg Camera at beam line BL6A2 at the Photon Factory, Tsukuba (Sakabe, 1991). The data were processed using WEIS (Higashi, 1989; Fields et al., 1992) yielding 29,729 unique reflections of 106,232 total data collected with an R_{merge} of 0.090 (mean R_{sym} of 0.078; 63% complete to 1.8 Å; R_{merge} for a 1.6–1.8-Å shell was 0.170). Native Tern N9 data were also collected to 2.0 Å on an *R*-axis detector for comparison, yielding 28,540 unique data from two data sets (each with a merging *R*-factor of 0.07 and a combined merging *R*-factor of 0.012, 66% complete to 2 Å; R_{merge} for a 2.2–2-Å shell was 0.175). The completeness of data as a function of resolution of the two data sets is shown on Figure 8. All data less than 1σ for the Photon Factory data and 2σ for the *R*-axis data were rejected from the analysis.

Refinement

A model for 4-guanidino-Neu5Ac2en was built into a difference Fourier map using the phases (to 2.5 Å) from the refined native data for N9 (Tulip et al., 1991). The model was then refined by X-PLOR (Brünger, 1992), extending the data to 1.8 Å. A cycle of simulated annealing was carried out followed by several cycles of energy and temperature factor refinement with manual intervention using the graphics program O (Jones et al., 1991) to locate additional water molecules (these were located by examining peaks in the $F_o - F_c$ maps that were above 5σ) and to correct minor errors in the positions of side chains. All charges on the 2-carboxylate and the 4-guanidino group were set to zero, as were the charges of all amino acid side chains. The final *R*-factor is 0.156, for data from 6 to 1.8 Å, using the energy restraints of Engh and Huber (1991) with RMS deviations from ideal bonds and angles of 0.010 Å and 1.66°. A similar strategy was employed for the refinement of the native data resulting in a final *R*-factor of 0.152 for data from 6 to 2 Å and RMS deviation from ideal of bonds and angles of 0.010 Å and 1.8°. A

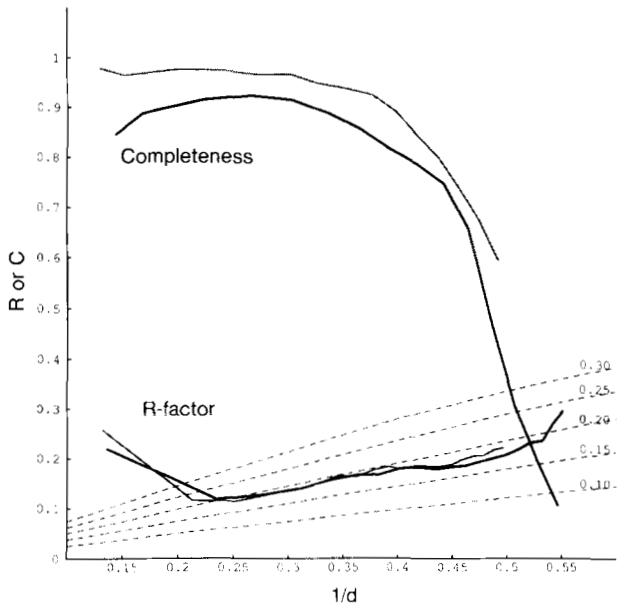

Fig. 8. Completeness of X-ray data and the final *R*-factors of the refined atomic model as a function of resolution ($1/d$, where d is the resolution in Å). The bold and shaded lines represent the Tern/N9 4-guanidino-Neu5Ac2en complex and the Tern/N9 native data, where the data limits are 1.8 Å and 2.0 Å, respectively. Dashed lines represent the Luzzati error contours from 0.1 to 0.3 Å in steps of 0.05 Å.

Luzzati plot (Luzzati, 1952) of the refined native inhibitor complex and sialic acid complex structure indicates a coordinate error of between 0.20 and 0.15 Å for the native and the inhibitor complex (Fig. 8), and the RMS difference between the native and the inhibitor complex structures is 0.25 Å for all atoms. The coordinates of the two structures have been deposited in the Brookhaven Protein Data Bank (codes 7NN9 and 1NNC).

Theoretical calculations

The energy minimizations were carried out with Amber v4.0 (Pearlman et al., 1990), using the molecular mechanics parameters file parm91.dat in Amber4 and amber.frc in InsightII (v.2.3.0) program (Biosym Technologies, San Diego). The partial charges for the atoms in 4-guanidino-Neu5Ac2en were derived by fitting electrostatic potentials calculated with the semiempirical molecular orbital method MNDO using MOPAC 6.0 (Stewart, 1990). The N- and C-termini of neuraminidase were kept in their ionic form. Amino acid residues lysine, arginine, glutamic acid, and aspartic acid side chains were charged, whereas histidines were protonated at the ϵ position.

Two different starting models were used: first, the X-ray model and second, the model in which 4-guanidino group of the inhibitor was rotated about the C4–N bond such that the dihedral angle was increased from 172° (in the refined X-ray structure) to 220°. This change allows H-bonding between the 4-guanidino group and both Glu 119 and Glu 227, whereas the X-ray result does not permit such an interaction with Glu 119. Each starting structure was prepared by solvating a "cap" of 124 TIP3P (Jorgensen et al., 1983) water molecules within a radius of 18 Å centered on the C4 carbon of 4-guanidino-Neu5Ac2en; in addition, the crystallographically ordered wa-

ters were included. The system was minimized under conditions of a distance-dependent dielectric constant of $1.0 * r$ and a cut-off for nonbonded interactions of 15 Å. First the cap of water was relaxed, followed by the gradual relaxing of constraints on the neuraminidase and the 4-guanidino-Neu5Ac2en heavy atom positions (constraints being reduced $100 \rightarrow 50 \rightarrow 15 \rightarrow 2 \rightarrow 0$ kcal mol^{-1} $Å^{-1}$). The minimization was terminated when the norm of the gradient of the energy dropped below 0.01 kcal mol^{-1} $Å^{-1}$.

The procedure was repeated for both starting models, but now with the protein non-hydrogen atoms "frozen" at their X-ray positions. After the initial relaxation of the solvent cap, only the amino acid and water hydrogens were allowed to move, and the constraints on the 4-guanidino-Neu5Ac2en heavy atoms were relaxed gradually as before.

Acknowledgments

We thank J. McKimm-Breschkin, J. Caldwell, and A. Kortt for providing material for crystallization; M. von Itzstein and W. Wu for the inhibitor; A. van Donkelaar and D. Marshall for technical assistance; P. Davis for computing assistance; Prof. Sakabe and K.E.K. for access to the Photon Factory, Tsukuba; and Biota Holdings Ltd., Glaxo Australia, and the Australian National Beam Line Facility for financial support.

References

Baker AT, Varghese JN, Laver WG, Air GM, Colman PM. 1987. The three-dimensional structure of neuraminidase of subtype N9 from an avian influenza virus. *Proteins Struct Funct Genet 1*:111-117.

Bossart-Whitaker P, Carson M, Babu YS, Smith CD, Laver WG, Air GM. 1993. Three-dimensional structure of influenza A N9 neuraminidase and its complex with the inhibitor 2-deoxy 2,3-dehydro-*N*-acetyl neuraminic acid. *J Mol Biol 232*:1069-1083.

Brünger AT. 1992. *X-PLOR, version 3.3: A system for X-ray crystallography and NMR*. New Haven, Connecticut: Yale University Press.

Burmeister WP, Ruigrok RWH, Cusack S. 1992. The 2.2 Å resolution crystal structure of influenza B neuraminidase and its complex to sialic acid. *EMBO J 11*:49-56.

Colman PM. 1989. Influenza virus neuraminidase—Enzyme and antigen. In: Krug RM, ed. *The influenza viruses*. New York: Plenum. pp 175-218.

Colman PM, Laver WG, Varghese JN, Baker AT, Tulloch PA, Air GM, Webster RG. 1987. Three-dimensional structure of a complex of antibody with influenza virus neuraminidase. *Nature 326*:358-363.

Colman PM, Tulip WR, Varghese JN, Tulloch PA, Baker AT, Laver WG, Air GM. 1989. 3-D structures of influenza virus neuraminidase-antibody complexes. *Proc R Soc Lond B 323*:511-518.

Colman PM, Varghese JN, Laver WG. 1983. Structure of the catalytic and antigenic sites in influenza virus neuraminidase. *Nature 303*:41-44.

Crennell SJ, Garman EF, Laver WG, Vimr ER, Taylor GL. 1993. Crystal structure of a bacterial sialidase (from *Salmonella typhimurium* LT2) shows the same fold as an influenza virus neuraminidase. *Proc Natl Acad Sci USA 90*:9852-9856.

Crennell S, Garman E, Laver G, Vimr E, Taylor G. 1994. Crystal structure of *Vibrio cholerae* neuraminidase reveals dual lectin-like domains in addition to the catalytic domain. *Structure 2*:535-544.

Engh RA, Huber R. 1991. Accurate bond and angle parameters for X-ray protein-structure refinement. *Acta Crystallogr A 47*:392-400.

Fields BA, Guss JM, Lawrence MC, Nakagawa A. 1992. The Weissenberg method for the collection of diffraction data from macromolecular crystals: Modifications to the data-processing program WEIS. *J Appl Crystallogr 25*:809-811.

Hart GJ, Bethell RC. 1995. 2-3-Didehydro-2-4-dideoxy-4-guanidino-*N*-acetyl-D-neuraminic acid (4-guanidino-Neu5Ac2en) is a slow-binding inhibitor of sialidase from both influenza A virus and influenza B virus. *Biochem Biophys Res Commun*. Forthcoming.

Hayden F, Lobo M, Esinhart J, Hussey E. 1994. Efficacy of 4-guanidino Neu5Ac2en in experimental human influenza A virus infection. *Abstracts, 34th ICAAC, Orlando, Florida*.

Higashi T. 1989. The processing of diffraction data taken on a screenless Weissenberg camera for macromolecular crystallography. *J Appl Crystallogr 21*:273-278.

Jones TA, Zou JY, Kjeldgaard M. 1991. Improved methods for building protein models in electron density maps and location of errors in these models. *Acta Crystallogr A 47*:110-119.

Jorgensen WL, Chandrasekhar J, Madura JD, Impey RW, Klein ML. 1983. Comparison of simple potential functions for simulating liquid water. *J Chem Phys 79*:926-935.

Laver WG, Colman PM, Webster RG, Hinshaw VS, Air GM. 1984. Influenza virus neuraminidase with haemagglutinin activity. *Virology 137*: 314-323.

Luzzati PV. 1952. Traitement statistique des erreurs dans la determination des structures cristallines. *Acta Crystallogr 5*:802-810.

McKimm-Breschkin JL, Caldwell JB, Guthrie RE, Kortt AA. 1991. A new method for the purification of influenza A virus. *J Virol Methods 32*:121-124.

Pearlman DA, Case DA, Caldwell J, Seibel G, Singh UC, Weiner PK, Kollman PA. 1990. *AMBER 4.0*. San Francisco, California: University of California.

Pegg MS, von Itzstein M. 1994. Slow-binding inhibition of sialidase from influenza virus. *Biochem Int 32*:851-858.

Sakabe N. 1991. X-ray diffraction data collection system for modern protein crystallography, with a Weissenberg camera and an imaging plate using synchrotron radiation. *Nucl Inst Methods Phys Res A 303*:448-465.

Stewart JJP. 1990. MOPAC: A semiempirical molecular orbital program. *J Comput-Aided Mol Des 4*:1-45.

Tulip WG, Varghese JN, Baker AT, van Donkelaar A, Laver WG, Webster RG, Colman PM. 1991. Refined atomic structures of N9 subtype influenza virus neuraminidase and escape mutants. *J Mol Biol 221*:487-497.

Varghese JN, Colman PM. 1991. Three-dimensional structure of the neuraminidase of influenza virus A/Tokyo/3/67 at 2.2 Å resolution. *J Mol Biol 221*:473-486.

Varghese JN, Laver WG, Colman PM. 1983. Structure of the influenza virus glycoprotein antigen neuraminidase at 2.9 Å resolution. *Nature 303*:35-40.

Varghese JN, McKimm-Breschkin JL, Caldwell JB, Kortt AA, Colman PM. 1992. The structure of the complex between influenza virus neuraminidase and sialic acid, the viral receptor. *Proteins 14*:327-332.

Varghese JN, Webster RG, Laver WG, Colman PM. 1988. The three-dimensional structure of an escape mutant of the neuraminidase of influenza virus A/Tokyo/3/67. *J Mol Biol 200*:201-203.

von Itzstein M, Wu WY, Kok GB, Pegg MS, Dyason JC, Jin B, Van Phan T, Symthe ML, White HF, Oliver SW, Colman PM, Varghese JN, Ryan DM, Woods JM, Bethell RC, Hotham VJ, Cameron JM, Penn CR. 1993. Rational design of potent sialidase-based inhibitors of influenza virus replication. *Nature 363*:418-423.